ANNALS of Faculty Engineering Hunedoara
International Journal of Engineering
ISSN: 1584 - 2673

EFFECTS OF FIRST ORDER CHEMICAL REACTION ON FLOW PAST AN OSCILLATING SEMI-INFINITE VERTICAL PLATE

A.R. VIJAYALAKSHMI , R. MUTHUCUMARASWAMY

Department of Applied Mathematics, Sri Venkateswara College of Engineering
Sriperumbudur 602 105, INDIA.

ABSTRACT
Effects of homogeneous chemical reaction of first order on unsteady flow past an oscillating semi-infinite vertical plate have been studied. The dimensionless governing equations are solved by an unconditionally stable and fast converging implicit finite difference scheme. The effect of velocity and temperature for different parameters like chemical reaction parameter, thermal Grashof number, mass Grashof number and time are studied. It is observed that due to the presence of first order chemical reaction, the velocity increases during generative reaction and decreases in destructive reaction.
Keywords: Chemical reaction, oscillating vertical plate, isothermal, heat transfer, mass diffusion.

1. INTRODUCTION

Chemical reactions can be codified as either heterogeneous or homogeneous processes. In well-mixed systems, the reaction is heterogeneous, if it takes place at an interface and homogeneous, if it takes place in solution. In most cases of chemical reactions, the reaction rate depends on the concentration of the species itself. In many chemical engineering processes, there does occur the chemical reaction between a foreign mass and the fluid in which the plate is moving. These processes take place in numerous industrial applications, e.g., polymer production, manufacturing of ceramics or glassware and food processing. Oscillating plate is used in cooling systems as heat exchangers.

Chambre and Young [1] have analyzed a first order chemical reaction in the neighbourhood of a horizontal plate. Das et al [3] have studied the effect of homogeneous first order chemical reaction on the flow past an impulsively started infinite vertical plate with uniform heat flux and mass transfer. Again, mass transfer effects on moving isothermal vertical plate in the presence of chemical reaction studied by Das et al [4]. The flow of a viscous, incompressible fluid past an infinite isothermal vertical plate, oscillating in its own plane, was solved by Soundalgekar [5]. Soundalgekar et al[6] derived an exact solution for the effect of mass transfer on the flow past an infinite vertical oscillating plate in the presence of constant heat flux. Mass transfer effects on isothermal vertical oscillating plate in the presence of chemical reaction was solved analytically by Muthucumarasamy et al[7]. In all the above cases the dimensionless governing equations were solved by the Laplace-transform technique and the solutions are valid only at lower time level.

Analytical or numerical work on transient flow past an oscillating semi-infinite vertical plate under the combined buoyancy effects of heat and mass diffusion in the presence of chemical reaction has not received attention of any researcher. Hence, the present study is to investigate the flow past an oscillating semi-infinite vertical plate with homogeneous first order chemical reaction by an implicit finite-difference scheme of Crank-Nicolson type.

2. FORMULATION OF THE PROBLEM

Consider a laminar, unsteady natural convection flow of a viscous incompressible fluid past an oscillating semi-infinite vertical plate which is at rest and surrounds the plate with temperature T'_∞ and concentration C'_∞ It is assumed that there is a first order chemical reaction between the diffusing species and the fluid. Here, the x-axis is taken along the plate in the vertically upward direction and the y-axis is taken normal to the plate. Initially, it is assumed that the plate and the fluid are of the same temperature and concentration. At time $t'>0$, the plate starts oscillating in its own plane with frequency ω' and the temperature of the plate and the concentration level are also raised linearly with time. Then by usual Boussinesq's approximation, the unsteady flow is governed by the following equations**:**

$$\frac{\partial u}{\partial x}+\frac{\partial v}{\partial y}=0 \tag{1}$$

$$\frac{\partial u}{\partial t'}+u\frac{\partial u}{\partial x}+v\frac{\partial u}{\partial y}=g\beta(T'-T'_\infty)\ +\ g\beta^*(C'-C'_\infty)+\nu\frac{\partial^2 u}{\partial y^2} \tag{2}$$

$$\rho C_p\left(\frac{\partial T'}{\partial t'}+u\frac{\partial T'}{\partial x}+v\frac{\partial T'}{\partial y}\right)=\frac{\partial^2 T'}{\partial y^2} \tag{3}$$

$$\frac{\partial C'}{\partial t'}+u\frac{\partial C'}{\partial x}+v\frac{\partial C'}{\partial y}=D\frac{\partial^2 C'}{\partial y^2}-K_1 C' \tag{4}$$

The initial and boundary conditions are

$$\begin{aligned}
&t'\le 0: && u=0, && v=0, && T'=T'_\infty, && C'=C'_\infty && \\
&t'>0: && u=u_0\cos\omega' t', && v=0, && T'=T'_w, && C'=C'_w && \text{at } y=0\\
& && u=0, && && T'=T'_\infty, && C'=C'_\infty && \text{at } x=0\\
& && u\to 0, && && T\to T'_\infty, && C'\to C'_\infty && \text{as } y\to\infty
\end{aligned} \tag{5}$$

On introducing the following non-dimensional quantities:

$$X=\frac{xu_0}{\nu},\ Y=\frac{yu_0}{\nu},\ U=\frac{u}{u_0},\ V=\frac{v}{u_0},\ \omega=\frac{\omega'\nu}{u_0^2}, \tag{6}$$

$$t=\frac{t'u_0^2}{\nu},\ T=\frac{T'-T'_\infty}{T'_w-T'_\infty},\ Gr=\frac{\nu g\beta(T'_w-T'_\infty)}{u_0^3},\ Pr=\frac{\nu}{\alpha},$$

$$C=\frac{C'-C'_\infty}{C'_w-C'_\infty},\ Gc=\frac{\nu g\beta^*(C'_w-C'_\infty)}{u_0^3},\ Sc=\frac{\nu}{D},\ K=\frac{\nu K_1}{u_0^2}$$

equations (1) to (4) are reduced to the following non-dimensional form

$$\frac{\partial U}{\partial X}+\frac{\partial V}{\partial Y}=0 \tag{7}$$

$$\frac{\partial U}{\partial t}+U\frac{\partial U}{\partial X}+V\frac{\partial U}{\partial Y}=Gr\ T+Gc\ C+\frac{\partial^2 U}{\partial Y^2} \tag{8}$$

$$\frac{\partial T}{\partial t}+U\frac{\partial T}{\partial X}+V\frac{\partial T}{\partial Y}=\frac{1}{Pr}\frac{\partial^2 T}{\partial Y^2} \tag{9}$$

$$\frac{\partial C}{\partial t}+U\frac{\partial C}{\partial X}+V\frac{\partial C}{\partial Y}=\frac{1}{Sc}\frac{\partial^2 C}{\partial Y^2}-KC \tag{10}$$

The corresponding initial and boundary conditions in non-dimensional quantities are

$$\begin{aligned}
&t\le 0: && U=0, && V=0, && T=0, && C=0 && \\
&t>0: && U=1, && V=0, && T=1, && C=1 && \text{at } Y=0\\
& && U=0, && && T=0, && C=0, && \text{at } X=0\\
& && U\to 0, && && T\to 0, && C\to 0 && \text{as } Y\to\infty
\end{aligned} \tag{11}$$

A reaction is said to be of the order n, if the reaction rate if proportional to the n^{th} power of the concentration. In particular, a reaction is said to be first order, if the rate of reaction is directly proportional to concentration itself. Such a study is found useful in chemical processing industries such as fibre drawing, crystal pulling from the melt and polymer production.

3. NUMERICAL TECHNIQUE

In order to solve these unsteady, non-linear coupled equations (7) to (10) under the conditions (11), an implicit finite difference scheme of Crank-Nicolson type has been employed. The finite difference equations corresponding to equations (7) to (10) are as follows:

$$\frac{\left[U_{i,j}^{n+1}-U_{i-1,j}^{n+1}+U_{i,j}^{n}-U_{i-1,j}^{n}+U_{i,j-1}^{n+1}-U_{i-1,j-1}^{n+1}+U_{i,j-1}^{n}-U_{i-1,j-1}^{n}\right]}{4\Delta X}+\frac{\left[V_{i,j}^{n+1}-V_{i,j-1}^{n+1}+V_{i,j}^{n}-V_{i,j-1}^{n}\right]}{2\Delta Y}=0 \tag{12}$$

$$\frac{\left[U_{i,j}^{n+1}-U_{i,j}^{n}\right]}{\Delta t}+U_{i,j}^{n}\frac{\left[U_{i,j}^{n+1}-U_{i-1,j}^{n+1}+U_{i,j}^{n}-U_{i-1,j}^{n}\right]}{2\Delta X}+V_{i,j}^{n}\frac{\left[U_{i,j+1}^{n+1}-U_{i,j-1}^{n+1}+U_{i,j+1}^{n}-U_{i,j-1}^{n}\right]}{4\Delta Y}$$

$$= \frac{Gr}{2}\left[T_{i,j}^{n+1} + T_{i,j}^{n}\right] + \frac{Gc}{2}\left[C_{i,j}^{n+1} + C_{i,j}^{n}\right] + \frac{\left[U_{i,j-1}^{n+1} - 2U_{i,j}^{n+1} + U_{i,j+1}^{n+1} + U_{i,j-1}^{n} - 2U_{i,j}^{n} + U_{i,j+1}^{n}\right]}{2(\Delta Y)^2} \quad (13)$$

$$\frac{\left[T_{i,j}^{n+1} - T_{i,j}^{n}\right]}{\Delta t} + U_{i,j}^{n}\frac{\left[T_{i,j}^{n+1} - T_{i-1,j}^{n+1} + T_{i,j}^{n} - T_{i-1,j}^{n}\right]}{2\Delta X} + V_{i,j}^{n}\frac{\left[T_{i,j+1}^{n+1} - T_{i,j-1}^{n+1} + T_{i,j+1}^{n} - T_{i,j-1}^{n}\right]}{4\Delta Y}$$

$$= \frac{1}{Pr}\frac{\left[T_{i,j-1}^{n+1} - 2T_{i,j}^{n+1} + T_{i,j+1}^{n+1} + T_{i,j-1}^{n} - 2T_{i,j}^{n} + T_{i,j+1}^{n}\right]}{2(\Delta Y)^2} \quad (14)$$

$$\frac{\left[C_{i,j}^{n+1} - C_{i,j}^{n}\right]}{\Delta t} + U_{i,j}^{n}\frac{\left[C_{i,j}^{n+1} - C_{i-1,j}^{n+1} + C_{i,j}^{n} - C_{i-1,j}^{n}\right]}{2\Delta X} + V_{i,j}^{n}\frac{\left[C_{i,j+1}^{n+1} - C_{i,j-1}^{n+1} + C_{i,j+1}^{n} - C_{i,j-1}^{n}\right]}{4\Delta Y}$$

$$= \frac{1}{Sc}\frac{\left[C_{i,j-1}^{n+1} - 2C_{i,j}^{n+1} + C_{i,j+1}^{n+1} + C_{i,j-1}^{n} - 2C_{i,j}^{n} + C_{i,j+1}^{n}\right]}{2(\Delta Y)^2} - \frac{K}{2}\left(C_{i,j}^{n+1} + C_{i,j}^{n}\right) \quad (15)$$

Here the region of integration is considered as a rectangle with sides $X_{max}(=1)$ and $Y_{max}(=3)$, where Y_{max} corresponds to $Y=\infty$ which lies very well outside both the momentum and energy boundary layers. The maximum of Y was chosen as 3 after some preliminary investigations so that the last two of the boundary conditions (11) are satisfied with in the tolerance limit 10^{-5}.

After experimenting with a few set of mesh sizes, the mesh sizes have been fixed at the level $\Delta X = 0.05$, $\Delta Y = 0.25$ with time step $\Delta t = 0.01$. In this case, the spatial mesh sizes are reduced by 50% in one direction, and later in both directions, and the results are compared. It is observed that, when the mesh size is reduced by 50% in the Y-direction, the results differ in the fifth decimal place while the mesh sizes are reduced by 50% in X-direction or in both directions, the results are comparable to three decimal places. Hence, the above mesh sizes have been considered as appropriate for calculation. The coefficients $U_{i,j}^{n}$ and $V_{i,j}^{n}$ appearing in the finite-difference equations are treated as constants in any one time step. Here i-designates the grid point along the X-direction, j along the Y-direction and k to the t-time. The values of U, V and T are known at all grid points at $t=0$ from the initial conditions.

The computations of U, V, T and C at time level $(n+1)$ using the values at previous time level (n) are carried out as follows: The finite difference Equation (15) at every internal nodal point on a particular i-level constitute a tridiagonal system of equations. Such a system of equations are solved by using Thomas algorithm as discussed in Carnahan *et al.* [2]. Thus, the values of C are found at every nodal point for a particular i at $(n+1)^{th}$ time level. Similarly, the values of T are calculated from Equation (14). Using the values of C and T at $(n+1)^{th}$ time level in the equation (13), the values of U at $(n+1)^{th}$ time level are found in a similar manner. Thus, the values of C, T and U are known on a particular i-level. Finally, the values of V are calculated explicitly using the Equation (12) at every nodal point on a particular i-level at $(n+1)^{th}$ time level. This process is repeated for various i-levels. Thus the values of C, T, U and V are known, at all grid points in the rectangular region at $(n+1)^{th}$ time level.

In a similar manner computations are carried out by moving along the i-direction. After computing values corresponding to each i at a time level, the values at the next time level are determined in a similar manner. Computations are repeated until the steady-state is reached. The steady-state solution is assumed to have been reached, when the absolute difference between the values of U, as well as temperature T and concentration C at two consecutive time steps are less than 10^{-5} at all grid points.

The finite difference scheme is unconditionally stable. The local truncation error is $O(\Delta t^2 + \Delta Y^2 + \Delta X)$ and it tends to zero as $\Delta t, \Delta X$ and ΔY tend to zero. Hence the scheme is compatible. Stability and compatibility ensures convergence

4. RESULTS AND DISCUSSION

Representative numerical results for the uniform heat and mass diffusion will be discussed in this section. The mass diffusion equation (10) can be adjusted to meet these circumstances if one

takes(i) $K > 0$ for the destructive reaction, (ii) $K < 0$ for the generative reaction and (iii) $K = 0$ for no reaction.

The velocity profiles for different phase angles ($\omega t = \pi/6, \pi/4, \pi/3, \pi/2$), Gr=5, Gc=5, Sc=0.6, Pr=0.71 and t=0.2 are shown in Fig. 1. It is observed that the velocity increases with decreasing phase angle. This shows that velocity decreases in the presence of high oscillation.

The velocity for different chemical reaction parameter(K=-5,-2,0,0.2,2), $\omega t = \pi/6$, Gr=5, Gc=5, Pr=0.71, Sc=0.6 and Pr=0.71 are shown in Fig. 2. It is observed that the velocity increases with decreasing chemical reaction parameter. This shows that the velocity increases during generative reaction and decreases in destructive reaction. The time taken to reach the steady-state increases with increasing chemical reaction parameter. This shows that the contribution of mass diffusion to the buoyancy force increases the maximum velocity significantly.

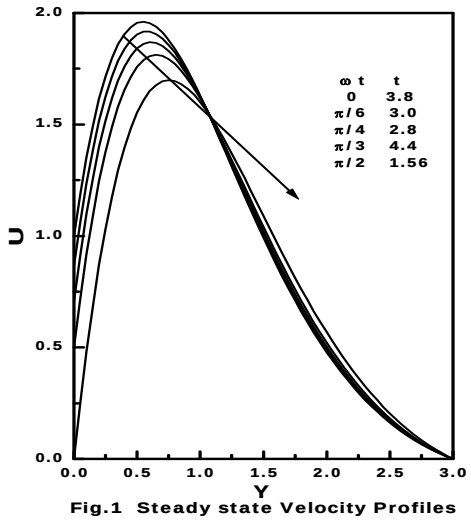

Fig.1 Steady state Velocity Profiles for different ωt

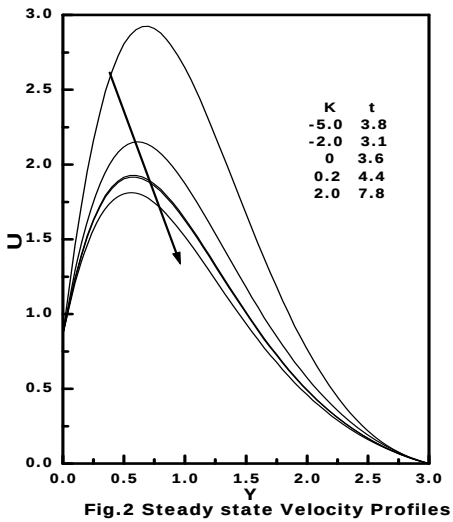

Fig.2 Steady state Velocity Profiles for different K

The steady state velocity profiles for different values of the thermal Grashof number, mass Grashof number is shown in Fig. 3. It is observed that the velocity increases with increasing thermal Grashof number or mass Grashof number. As thermal Grashof number or mass Grashof number increases, the buoyancy effect becomes more significant, it implies that, more fluid is entrained from the free stream due to the strong buoyancy effects as Gr or Gc increases.

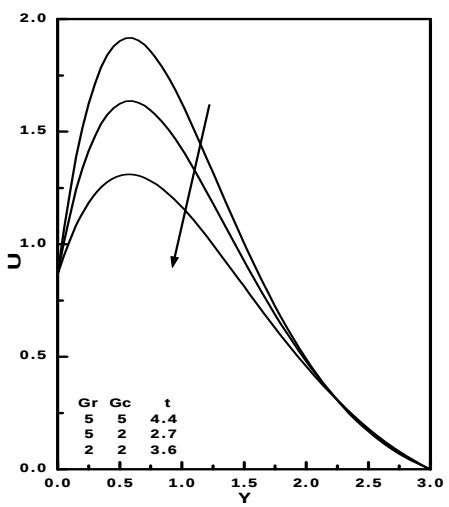

Fig.3. Steady state velocity profiles at X=1.0 for different Gr,Gc

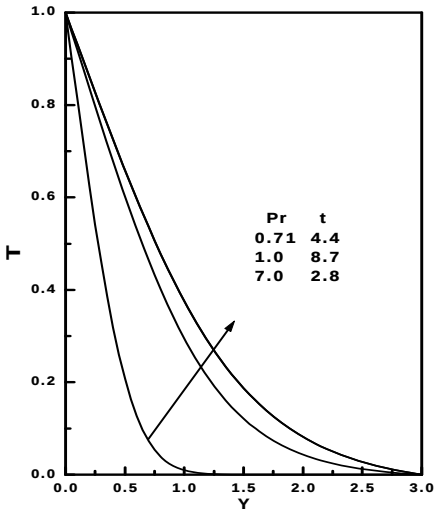

Fig.4. Steady state temperature profiles at X=1.0 for different Pr

Fig. 4 represents the temperature profiles for different values of the Prandtl number. The effect of the prandtl number plays a significant role in temperature field. It is observed that there is a fall in temperature with increasing the Prandtl number.

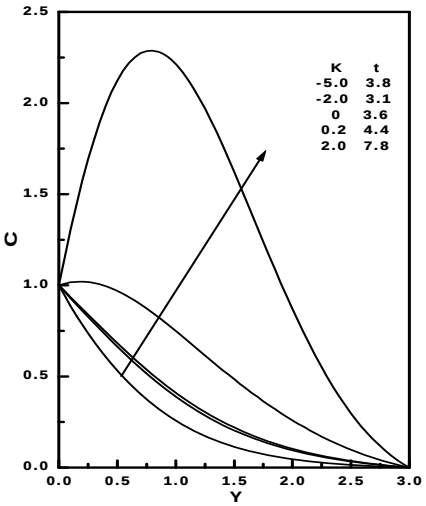

Fig.5. Concentration profiles at X=1.0 for different K

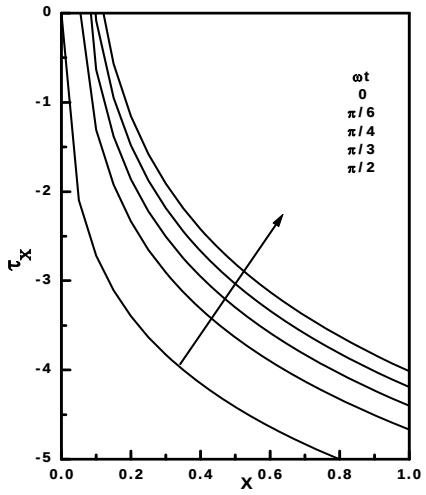

Fig.6. Local skin friction for different ωt

The concentration profiles for different values of the the chemical reaction parameter (K=-5,-2,0,0.2,2,Sc=0.6) are exhibited in Fig. 5. The wall concentration increases during generative reaction and decreases during destructive reaction. It is observed that there is a fall in concentration due to increasing the values of the chemical reaction parameter.

Knowing the velocity, the temperature and the concentration field, it is customary to study the skin-friction, the rate of heat transfer and the rate of concentration in their transient and steady-state conditions. The dimensionless local as well as average values of the skin-friction, the Nusselt number and the Sherwood number are given by the following expressions:

$$\tau_X = -\left(\frac{\partial U}{\partial Y}\right)_{Y=0} \tag{16}$$

$$\bar{\tau} = -\int_0^1 \left(\frac{\partial U}{\partial Y}\right)_{Y=0} dX \tag{17}$$

$$Nu_X = -X\left[\frac{\left(\frac{\partial T}{\partial Y}\right)_{Y=0}}{T_{Y=0}}\right] \tag{18}$$

$$\overline{Nu} = -\int_0^1 \left[\frac{\left(\frac{\partial T}{\partial Y}\right)_{Y=0}}{T_{Y=0}}\right] dX \tag{19}$$

$$Sh_X = -X\left(\frac{\partial C}{\partial Y}\right)_{Y=0} \tag{20}$$

$$\overline{Sh} = -\int_0^1 \left(\frac{\partial C}{\partial Y}\right)_{Y=0} dX \tag{21}$$

The derivatives involved in the Equations (16) to (21) are evaluated using five-point approximation formula and then the integrals are evaluated using Newton-Cotes closed integration formula.

The local skin-friction values are evaluated from equation (16) and plotted in Fig. 6 as a function of the axial coordinate X. Localskin-friction decreases as X increases. The local wall shear stress increases with decreasing values of phase angles ωt The local Nusselt number for different phase angles ωt are shown in Fig. 7. The rate of heat transfer decreases with increasing phase angles ωt .

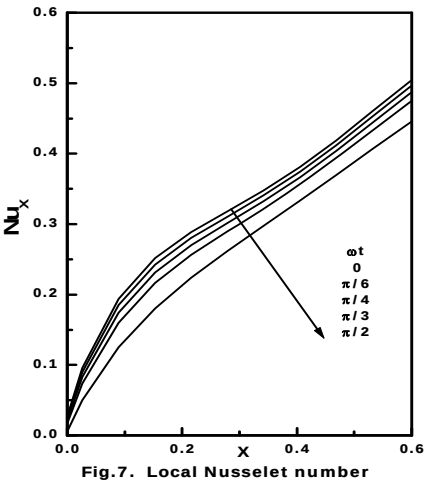

Fig.7. Local Nusselet number for different ωt

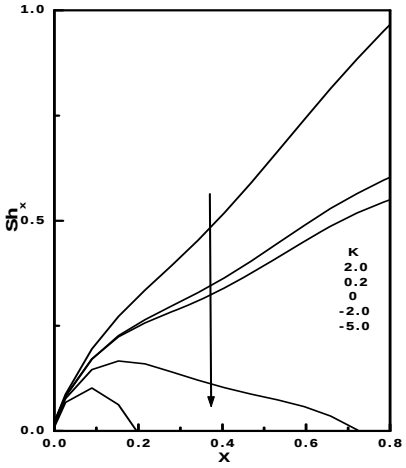

Fig.8. Local Sherwood number for different K

The Local Sherwood number for different values of the chemical reaction parameter are shown in Fig. 8. The local Sherwood number increases with increasing chemical reaction parameter.

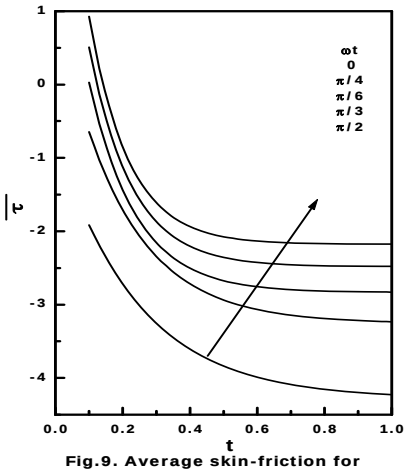

Fig.9. Average skin-friction for different ωt

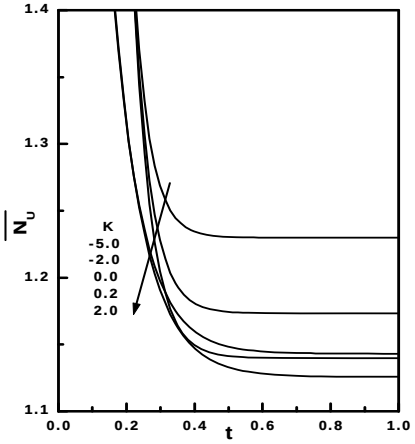

Fig.10. Average Nusselet number for different K

The average values of the skin-friction, Nusselt number and Sherwood number are shown in Fig. 9, 10, 11 and 12 respectively. The effects of the phase angles ωt on the average values of the skin-friction are shown in Fig. 9. The average skin-friction decreases with increasing phase angles ωt . The effects of the phase angles ωt , chemical reaction parameter K on the average values of the Nusselt number are shown in Fig. 10, 11 respectively. The average Nusselt number decreases with increasing phase angles ωt or increasing chemical reaction parameter.

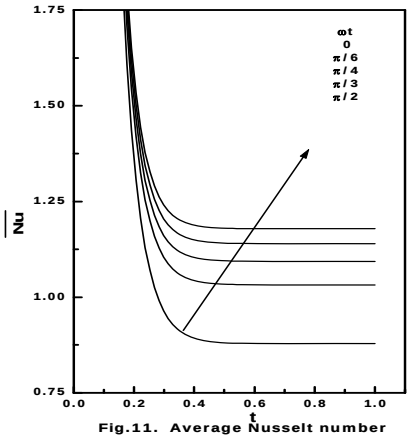

Fig.11. Average Nusselt number for different ωt

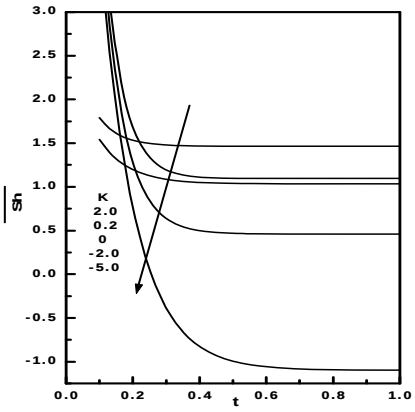

Fig.12. Average Sherwood number for different K

Fig.12 shows the effect of chemical reaction parameter K on the average values of the average Sherwood number. The Sherwood number increase with increasing values of the chemical reaction parameter. It is also observed that the average sherwood number increases during destructive reaction and decreases with generative reaction.

5. CONCLUSION

Finite difference analysis has been carried out for unsteady flow past an oscillating semi-infinite vertical plate with uniform surface temperature and mass diffusion in the presence of homogeneous chemical reaction of first order. The dimensionless governing equations are solved by an implicit scheme of Crank-Nicolson type. The effect of velocity and temperature for different parameter are studied. The local as well as average skin-friction, Nusselt number and Sherwood number are shown graphically. It is observed that the contribution of mass diffusion to the buoyancy force increases the maximum velocity significantly. It is also observed that the velocity decreases in the presence of chemical reaction. The study shows that the number of time steps to reach steady-state depends strongly on the chemical reaction parameter and phase angle. This shows that the velocity increases during generative reaction and decreases in destructive reaction. It was observed that the heat transfer performance of an oscillating plate is at constant rate.

Nomenclature

A ,a - constant
C' - concentration $\mathbf{mol.m^{-3}}$
C - dimensionless concentration
C_p - specific heat at constant pressure $\mathbf{J.kg^{-1}.K^{-1}}$
D - mass diffusion coefficient
erfc - complementary error function
g - acceleration due to gravity $\mathbf{m.s^{-2}}$
Gr - thermal Grashof number
Gc - mass Grashof number
k- thermal conductivity $\mathbf{J.m^{-1}.K^{-1}}$
K_l - chemical reaction parameter $\mathbf{J}$
K - dimensionless chemical reaction parameter
Pr - Prandtl number
Sc - Schmidt number
T - temperature of the fluid near the plate $\mathbf{K}$
t' - time $\mathbf{s}$
t - dimensionless time
u_0- amplitude of oscillation
u - velocity component in x-direction $\mathbf{m.s^{-1}}$
U - dimensionless velocity component in x-direction
x - spatial coordinate along the plate
y - spatial coordinate normal to the plate $\mathbf{m}$
Y - dimensionless coordinate axis normal to the plate

Greek symbols

β - volumetric coefficient of thermal expansion $\mathbf{K^{-1}}$
β' - volumetric coefficient of expansion with concentration $\mathbf{K^{-1}}$
η - similarity parameter
μ - coefficient of viscosity $\mathbf{Pa.s}$
ν - kinematic viscosity $\mathbf{m^2.s^{-1}}$
ωt - Phase angle $\mathbf{rad}$
ρ - density of the fluid $\mathbf{kg.m^{-3}}$
τ - dimensionless skin-friction
θ - dimensionless temperature

Subscripts

w - conditions at the wall
∞ - conditions in the free stream

REFERENCES

[1] P.L. Chambre, J.D. Young , On the diffusion of a chemically reactive species in a laminar boundary layer flow, The Physics of Fluids Vol. 1,pp. 48-54,1958.
[2] Carnahan B., Luther H.A. and Wilkes J.O., Applied Numerical Methods, John Wiley and Sons, New York, 1969.
[3] Das U.N., Deka R.K. and Soundalgekar V.M., Effects of mass transfer on flow past an impulsively started infinite vertical plate with constant heat flux and chemical reaction-Forschung im Ingenieurwesen, Vol. 60, pp. 284-287,1994.
[4] Das U.N., Deka R.K. and Soundalgekar V.M., Effects of mass transfer on flow past an impulsively started infinite vertical plate with chemical reaction- The Bulletin of GUMA, Vol. 5, pp. 13-20,1999.
[5] Soundalgekar V.M, Free Convection Effects on the Flow Past a Vertical Oscillating Plate, Astrophysics Space Science vol.64 , pp. 165-172, 1979.
[6] Soundalgekar V.M, Lahurikar R.M, Pohanerkar S.G., Birajdar N.S., Effects of Mass Transfer on the Flow Past an Oscillating Infinite Vertical Plate with Constant Heat Flux, Thermophysics and AeroMechanics, Vol. 1, pp. 119-124,1994.
[7] Muthcumarasamy R. and Janakiraman B.(2008), Mass transfer effects on isothermal vertical oscillating Plate in the presence of chemical reaction, Int.J.of Appl.Math. and Mech., Vol. 4(1), pp. 66-74.